Experimental Cell Research 400 (2021) 112490

Contents lists available at ScienceDirect

Experimental Cell Research

journal homepage: www.elsevier.com/locate/yexcr

Research article

Simultaneously characterization of tumoral angiogenesis and vasculogenesis in stem cell-derived teratomas

Michela Corsini [a,c,**], Cosetta Ravelli [a,c], Elisabetta Grillo [a], Patrizia Dell'Era [a,b], Marco Presta [a], Stefania Mitola [a,c,*]

[a] Department of Molecular and Translational Medicine, Via Branze 39, 25123, Brescia, University of Brescia, Italy
[b] cFRU Lab, Università degli Studi di Brescia, Viale Europa 11, 25123, Brescia, Italy
[c] Laboratory for Preventive and Personalized Medicine (MPP Lab), University of Brescia, Italy

ARTICLE INFO

Keywords:
Embryonic Stem Cells
Teratoma
Angiogenesis
Vasculogenesis
Chick embryo CAM

ABSTRACT

Tumor neovascularization may occur via both angiogenic and vasculogenic events. In order to investigate the vessel formation during tumor growth, we developed a novel experimental model that takes into account the differentiative and tumorigenic properties of Embryonic Stem cells (ESCs). Leukemia Inhibitory Factor-deprived murine ESCs were grafted on the top of the chick embryo chorionallantoic membrane (CAM) *in ovo*. Cell grafts progressively grew, forming a vascularized mass within 10 days. At this stage, the grafts are formed by cells with differentiative features representative of all three germ layers, thus originating teratomas, a germinal cell tumor. In addition, ESC supports neovascular events by recruiting host capillaries from surrounding tissue that infiltrates the tumor mass. Moreover, immunofluorescence studies demonstrate that perfused active blood vessels within the tumor are of both avian and murine origin because of the simultaneous occurrence of angiogenic and vasculogenic events. In conclusion, the chick embryo ESC/CAM-derived teratoma model may represent a useful approach to investigate both vasculogenic and angiogenic events during tumor growth and for the study of natural and synthetic modulators of the two processes.

1. Introduction

In physiologic and pathologic conditions, tissue vascularization may occur via vasculogenesis and angiogenesis. During embryonic development, the first functional organs to develop are blood vessels and the hematopoietic system. The vascular plexus is initially generated through *de novo* production and differentiation of endothelial cells (ECs) from angioblasts, a process known as vasculogenesis. Subsequently, the expansion and remodeling of this initial endothelial network occur through a second process known as angiogenesis [1]. Similarly, several evidence show that tumor vessels derive from the proliferation and migration of ECsin pre-existing vessels, and from the differentiation into ECs of bone-marrow-derived endothelial progenitor cells [2] or directly from the trans differentiation of tumoral cells [3,4].

Several model systems for experimental embryological studies have been developed. Among these, zebrafish and chick embryos have been mostly used [5–8]. Although their development is extremely rapid, 5 days post fertilization (dpf) and 21 dpf respectively, both models well recapitulate the development of human embryos, sharing molecular, cellular, and anatomical similarities with the human counterpart. In particular, the mechanism driving the assembly of new vessels is highly conserved in these model systems and humans [9].

The chick embryo shows several peculiarities: the ease of handling, with high capacity of observation and planar structures accessible throughout 21 days of development; the ease of labeling cells and tissues and the possibility of characterization of the extra-embryonic annexes, including the chorioallantoic membrane (CAM) [10]. All these features make the chick embryo a perfect (appropriate) model for the dynamic analysis of the evolution from one-cell stage to birth directly *in ovo* by live microscopy [11].

The chick CAM derives from the fusion of chorion and allantois, two layers, one of ectodermal origin and one of endodermal origin

Abbreviations: Embryonic Stem Cells, (ESCs); chick embryo chorionallantoic membrane, (CAM); endothelial cells, (ECs); days post fertilization, (dpf); ESC embryoid bodies, (EBs); Hematoxylin & Eosin, (H&E); Leukemia Inhibitory Factor, (LIF).

* Corresponding author. Department of Molecular and Translational Medicine, Via Branze 39, 25123, Brescia, University of Brescia. Italy.
** Corresponding author. Department of Molecular and Translational Medicine, Via Branze 39, 25123, Brescia, University of Brescia. Italy.
E-mail addresses: michela.corsini@unibs.it (M. Corsini), stefania.mitola@unibs.it (S. Mitola).

https://doi.org/10.1016/j.yexcr.2021.112490
Received 18 September 2020; Received in revised form 2 December 2020; Accepted 11 January 2021
Available online 21 January 2021
0014-4827/

respectively, connected by mesodermal components [12]. Its development occurs from embryonic development day 3 (stage 18 of Hamburger and Hamilton) to day 10 pf. However the chick CAM is fully differentiated by day 13 [13].

Over the last two decades, an increasing interest in the CAM as a robust experimental platform to study blood vessels has been shown by specialists of multiple disciplines, including bioengineering, development, morphology, biochemistry, transplant biology, cancer research, and drug development [14–16]. The tissue composition and accessibility of the CAM for experimental manipulation makes it an attractive preclinical *in vivo* model for drug screening and studies of vascular growth. Several studies reported the engraftment of CAM with soluble stimuli [17–19], cells or tissue biopsies for the analysis of the angiogenic events at 6–10 dpf stage of development. At that stage, the immune system is not fully developed, and the conditions for graft rejection have not yet been established [20].

Embryonic stem cells (ESCs) derived from the inner cell mass of the blastocyst are pluripotent stem cells, characterized by self-renewal and the ability to differentiate in the three germ layers: ectoderm, endoderm, and mesoderm *in vitro* and in murine models *in vivo* [21–23]. Moreover, ESCs present the ability for self-renewal, prolonged proliferation *in vitro*, and lack contact inhibition of proliferation. All these characteristics are shared with cancer cells, but the presence of a normal karyotype requires the use of special culture conditions to maintain these features in ESCs [24]. Developmental studies with ESCs are usually performed *in vitro*, using the hanging drop technique [25,26], and *in vivo* protocols, where the injection [subcutaneous, or orthotopic] of ESCs in mice generates a tumor mass, identified as a germline tumor, named teratoma [27].

Murine teratoma is an encapsulated tumor with well-differentiated tissue or organ components that can be traced to derivatives of the three primordial germ layers, that requires from 3 to 8 weeks to originate a proper differentiation of the mass [28].

Here we propose the use of chick embryo CAM as a simple model to test the differentiation capacity of ESCs and to analyze the vasculogenic and angiogenic processes at the same time during tumor development. The engraftment of ESCs on top of the CAM produces a vascularized tumor mass with differentiated tissues derived from all germ layers. A mosaic of murine and avian ECs form the tumor vasculature, suggesting contemporary events of angiogenesis and vasculogenesis. Thus, the chick embryo CAM can be considered a useful model for the investigation of the molecular mechanisms driving vessel formation originated both by cell differentiation, including the tumoral events of vascular mimicry, and by the active recruitment of vessels from surrounding tissue. Moreover, the chick embryo CAM represents a natural bioscaffold able to improve ESC differentiation and an easy and low-cost model for drug screening.

2. Methods

2.1. Murine ESC culture

Murine 1122 *fgfr1*$^{+/-}$ ESCs (ESCs) ([29]) adapted to grow without feeder cells were maintained in DMEM (Life Technologies, Grand Island, NY) supplemented with 20% fetal bovine serum (Lonza), 0.1 mmol/L non-essential amino acids (Life Technologies), 1 mmol/L sodium pyruvate (Life Technologies), 0.1 mmol/L β-mercaptoethanol (Sigma Aldrich), 2 mmol/L L-glutamine (Life Technologies), and where indicated also with 1000 U/mL mouse Leukemia Inhibitory Factor (LIF Chemicon, Millipore).

2.2. Embryoid body differentiation

To induce the differentiation, exponentially growing ESCs (400 cells) were resuspended in LIF-deprived medium and cultured in 30 μl hanging drops (T0) for 2 days to allow cell aggregation. Then, aggregates were transferred onto 0.5% agarose-coated dishes and grown for 5 days in DMEM. On day 7 (T7), ESC embryoid bodies (EBs) were transferred into 15 μ-slide 8 well (iBiDi) chambers and allowed to adhere. Adherent EBs were cultured in LIF-deprived medium for 3 days until T10. EBs were fixed in a 4% paraformaldehyde solution in PBS (PFA 4%) and stained.

2.3. CAM treatment

White Leghorn eggs were incubated at 37°C in a humidified incubator. At day 4 post incubation (p.i.) the shells were covered with a transparent adhesive tape and a small window sawed with scissors [30]. At day 7 p.i., drilled plastic coverslips were positioned on the surface of the CAM in a well vascularized area. $2x10^6$ LIF-deprived ESCs were transferred in the hole of the coverslips, in close contact with the exposed CAM. To facilitate cell engraftment, CAM in the bounded area was gently wounded before cell seeding. At different time points, samples were harvested from CAM and analyzed.

2.4. Immunohistochemistry

For histological characterization, ESC-derived teratomas were fixed overnight in zinc fixative or PFA 4% at 4°C, dehydrated in a grade alcohol series (50–100%) and embedded in paraffin. Paraffin-embedded samples were sectioned at a thickness of 4.0 μm, dewaxed, hydrated, and stained with Hematoxylin & Eosin (H&E), or May Grunwald & Giemsa solutions or processed for immunohistochemistry with anti-mouse Cytokeratin-19 (Santa Cruz Biotechnologies), anti-mouse N-cadherin (Santa Cruz Biotechnologies), anti-mouse Nestin (Santa Cruz Biotechnologies) antibodies.

To improve accessibility of antibodies to tissue antigens, tissue sections were incubated in Citrate Buffer Antigen Retrieval solution pH 6.0 at 95°C for 20 min before immunostaining. Positive signal was revealed by 3,3′-diaminobenzidine (DAB) (Roche). Sections were counterstained with Mayer's Hematoxylin before analysis by light microscopy. Images were acquired with a Zeiss Axio Imager.A2 Microscope equipped with 20 × EC Plan-NEOFLUAR and 40 × EC Plan-NEOFLUAR objectives. Image analysis was carried out using the open-source ImageJ software.

2.5. Immunofluorescence staining

For immunofluorescence analysis paraffin embedded tumor sections were stained with anti-VEGFR2 (Santa Cruz Biotechnologies), anti-human VWF (DakoCytomation) and anti-mouse PECAM1 (Santa Cruz Biotechnologies) antibodies followed by incubation with AlexaFluor 594-conjugated or AlexaFluor 488-conjugated secondary antibodies. Nuclei were counterstained with 4',6-diamidino,2-phenylindole (DAPI, Sigma). Tumor slices were analyzed using Confocal LSM510 microscope equipped with Plan-Neofluar 20 × /0.5 NA and Plan-Apochromat 63 × /1.4 NA oil objectives (Carl Zeiss). Z-stack images were elaborated using AxioVision Inside4D module (Carl Zeiss).

2.6. Gene expression

EBs and tumors were processed for the analysis of gene expression. A volume of Trizol® (according to the manufacturer's instruction) was added to EBs or ES-derived teratomas, and total RNA was extracted. Complementary DNA (cDNA) was made from 2 μg of total RNA using MML-V (Life Technologies). Real-time PCR was performed by ViiA7 Real-Time PCR System (Life Technologies), and data was analyzed with Viia7 Real-Time Software (Life Technologies). The oligonucleotide primers used for the amplification are listed in Table 1.

2.7. Data representation

Statistical analyses were performed using the statistical package Prism6 (GraphPad Software). Student's *t*-test for unpaired data (2-

Table 1
Real-Time PCR primers list.

Gene Name	Primers sequence (5'— 3')
Mm_Gapdh	For: CATGGCCTTCCGTGTTCCTAC
	Rev: TTGCTGTTGAAGTCGCAGGAG
Mm_Oct4	For: CAGGAGTTCAAGGGCAGCTTGT
	Rev: ATTAGGAGGAGGGGGTGCACAG
Mm_Nanog	For: CCTTCCCCTCGCCATCACACTGACA
	Rev:GAGGAAGGGCGAGGAGAGGCAGC
Mm_Sox2	For: CAAGGCAGAGAAGAGAGTGTTTGCA
	Rev:GCCGCCGCGATTGTTGTGAT
Mm_Nestin	For: TCTTGGCTTTCCTGACCCCA
	Rev: GGCTGTCACAGGAGTCTCAA
Mm_NeuroFilament2	For: TTCCCTCATATTGCACAAAGG
	Rev: AGACCTTTGAGGAGAAGCTGG
Mm_N Cadherin	For: GCAGTCTTACCGAAGGATGTG
	Rev: CCTGGGTTTCTTTGTCTTGG
Mm_Pax3	For: AAACCCAAGCAGGTGACAAC
	Rev: AGACAGCGTCCTTGAGCAAT
Mm_Snail1	For: CATCCTCGCTGGCATCTTCC
	Rev: GAGAGCCAAGCAGGAACCAG
Mm_Snai2	For: CTTTACCCAGTGGCCTTTCTC
	Rev: CCACAGATCTTGCAGACACAA
Mm_FoxA2	For: TTTAAACCGCCATGCACTCG
	Rev: ACGGAAGAGTAGCCCTCG
Mm_Glut1	For: GTGTATCCTGTTGCCCTTCTG
	Rev: CTGCCGACCCTCTTCTTTC
Mm_Prox1	For: CCTCAACATGCACTACAAC
	Rev: GGCATTGAAAAACTCCCGTA
Mm_Cxcr4	For: AGGAAACTGCTGGCTGAAA
	Rev: CACAGGCTATCGGGGTAAA
Mm_Lyve1	For: ACTCCTCGCCTCTATTTGGAC
	Rev: GCCTCGTTGGCTTCTGTG
Mm_Col1A1	For: GACCGATGGATTCCCGTTCG
	Rev: ACATTAGGCGCAGGAAGGTC
Mm_Wnt7a	For: GCAACCTGAGCGACTGTG
	Rev: CCCGCCTCGTTATTGTGTAA
Mm_Wnt7b	For: CGGAACTTAGGTAGCGTGGT
	Rev: TCGACTTTTCTCGTCGCTTT
Mm_CD31	For: AAGCCAAGGCCAAACAGA
	Rev: GGGTTTTACTGCATCATTTCC
Mm_Kdr	For: AGATGCCCGACTCCCTTT
	Rev: TTTCCCAGAGCAACACACC
Mm_Vcam	For: GAACTGATTATCCAAGTCTCTCCA
	Rev: CCATGTCTCCTGTCTTTGCTT
Mm_VE Cad	For: TTGGGCTTTCTGACTGTTGT
	Rev: CAGGGACTTCGTGGGTTT
Mm_BMP4	For: ATTCCTGGTAACCGAATGCTG
	Rev: CCGGTCTCAGGTATCAAACTAGC
Mm_CD34	For: CAGGAGAAAGGCTGGGTGAA
	Rev: GTTGTCTTGCTGAATGGCCG
Mm_CD45	For: TTGGATTTGCCCTTCTGG
	Rev: GGTGTAGGTGTTTGCCCTGT
Mm_Adiponectin	For: TGACGACACCAAAAGGGCTC
	Rev: CACAAGTTCCCTTGGGTGGA
Mm_AdipoR1	For: TCTTCGGGATGTTCTTCCTGG
	Rev: TTTGGAAAAAGTCCGAGAGACC
Mm_AdipoR2	For: GCCAAACACCGATTGGGGT
	Rev: GGCTCCAAATCTCCTTGGTAGTT
Gg_Gapdh	For: GCTAAGGCTGTGGGGAAAGT
	Rev: TCAGCAGCAGCCTTCACTAC
Gg_CD31	For: CGTGTTTATGCTCCAGTTTCCA
	Rev: AGTTTAGAGGCCTCCCCAGA

tailed) was used to test the probability of significant differences between two groups of samples. For more than two groups of samples, data were statistically analyzed with one-way ANOVA (analysis of variance), and individual group comparisons were evaluated by Bonferroni multiple comparison test. The significance level was set at $P < 0.05$.

3. Results

3.1. ES cells engraftment and growth on chick embryo CAM

Previous studies established the ability of murine ESCs to grow and differentiate into teratoma tumors when implanted subcutaneously in mice [31]. In compliance with the 3Rs rule applied to the use of animal models in the biological research, here we set up a protocol to test whether the chick embryo CAM can be a suitable natural scaffold able to support and promote ESC differentiation into teratoma tumors. To this, $2x10^6$ Leukemia Inhibitory Factor (LIF) -deprived ESCs were engrafted on the top of the CAM at day 7 of development. Considering the structure and the humidity of the CAM at this stage, we developed a system to confine and localize cells engrafted. To this aim, 13 mm diameter plastic coverslips were drilled with a rounded paper punch (5 mm diameter), sterilized under a UV lamp for 20 min, and placed onto the CAM close to a medium-sized blood vessel. To further facilitate the engraftment of ESCs, the CAM was gently brushed with a 200-μl tip, in order to induce the recruitment of inflammatory cells in the mesodermal layer (schematic representation in Fig. 1A). Brushing may cause a superficial wound, sometimes bleeding, on the CAM surface which quickly healed (Fig. 1B). May Grunwald Giemsa staining of a transversal CAM section shows the local inflammatory reaction that occurs in the wounded area of the CAM, characterized by the recruitment of monocyte/macrophage infiltrating cells (Fig. 1B bottom). In a pilot experiment, the implants were daily monitored using a zoom microscope and samples were harvested and weighed every two days up to day 10 (Fig. 1C–D). During the first 2 days, ESCs adhere to the CAM and form small and avascularized aggregates (Fig. 1C, black arrows) that rapidly grow during the next days of engraftment. The percentage of ESCs engraftment on the CAM is over 90%, and it is reduced to about 47% when cells are seeded in the absence of a wound (data not shown).

3.2. ESCs form a teratoma on chick embryo CAM

ESCs invade the epithelial layer and form a well-vascularized tissue inside the CAM tissue. At day 10, Hematoxylin & Eosin (H&E) staining of a tumor section clearly shows that ESCs (Fig. 2A), invade the chorion-derived epithelial layer and grow in the intermediate mesodermal layer, between the chorion and the allantois (Fig. 2A, red dashed lines). The reduced expression of *Oct4*, *Sox2*, and *Nanog* (Fig. 2B), as well as the presence of cells with different morphologies, metachromasia, and mitotic events, suggest the ability of chick embryo CAM to support not only the growth but also the differentiation of LIF-deprived ESCs. Samples were subjected to immunohistochemical analyses using antibodies against specific markers of the three germ layers. ESC-derived tumors display the presence of differentiated cells into disordered but recognizable tissue types. In particular, endoderm-derived tissues are represented by ciliated epithelium and by Cytokeratin-19 positive reaction (Fig. 2B–C). Mesoderm derived tissues are depicted by keratinized epithelium and by the expression of N-Cadherin (Fig. 2B–C). The presence of the ectodermal layer is featured by neural rosettes and by Nestin-positive cells (Fig. 2B–C). All these data support the evidence that ESCs implanted on chicken CAM form a tumoral mass with the characteristics of a teratoma similar to what previously described in murine models [31].

ESCs spontaneous differentiation is affected by the microenvironment, under the influence of paracrine stimuli, metabolic needs, or oxygen availability/deficiency [32,33]. In order to verify the ability of avian tissue to support and lead the differentiation of ESC into cell types of different origins, we compared the gene expression of teratomas grown on CAM with the gene expression of *in vitro* differentiated ESC.

As shown by the analysis of the stemness genes *Oct4*, *Nanog,* and *Sox2*, ESC-derived teratomas are more prone to lose stemness and differentiate when compared to EBs obtained by *in vitro* differentiation (Fig. 3). Then we analyzed the expression of genes related to endoderm-derived (*Prox1*, *Cxcr4*, *Glut1*, and *FoxA2),* mesoderm-derived (*CD31*, *VE Cad*, *BMP4*, and *Kdr)*, and ectoderm-derived (*Nestin*, *Neurofilament 2*, and *Pax3)* tissues. Genes that cannot be traced back to one specific lineage were also analyzed to further investigate the ESCs differentiation potential in CAM grafts *versus* EBs (Fig. 3). The results show similar

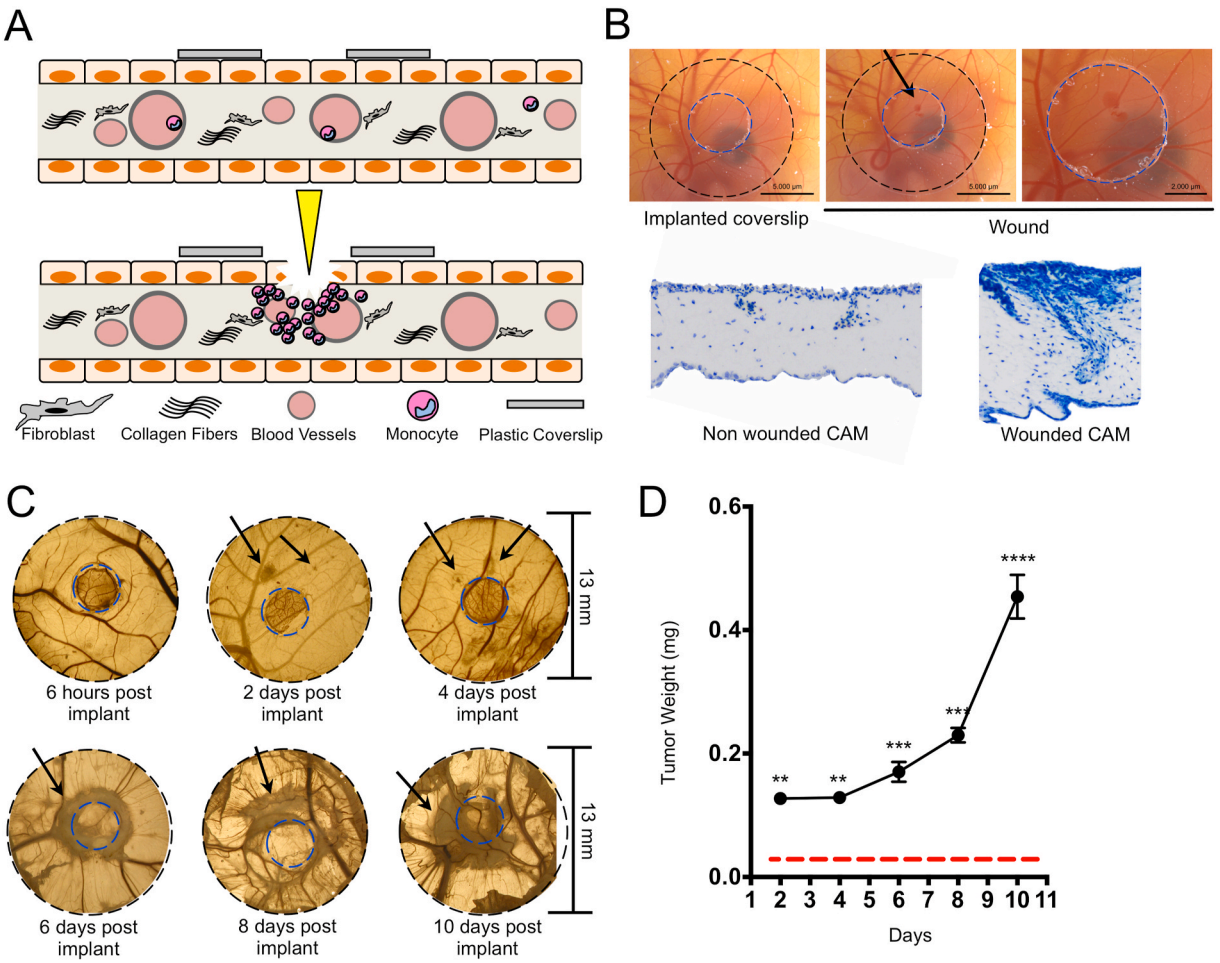

Fig. 1. ESC engraftment on chick embryo CAM. A) Basic infographic representation of a transversal section of CAM pre (top) and post (bottom) brush. B) View from above of the implanted plastic coverslip positioned on CAM surface, before and after brushing (black arrow). Black dashed lines represent the plastic coverslip (13 mm), and blue dashed lines represent the diameter of the punched hole (5 mm). After fixing, the coverslips were gently removed, and 4 μm Formalin Fixed Paraffin Embedded (FFPE) sections were stained with May Grunwald & Giemsa to confirm the recruitment of monocyte/macrophages in the brushed area. Samples were analyzed using a Zeiss Axio Imager.A2 microscope equipped with 20 × EC Plan-NEOFLUAR. C) Time course of $2x10^6$ ESCs implanted on brushed CAM. Samples were fixed, excised from eggs and photographed using a stereo zoom microscope AXIO Zoom.V16, from 6 h post-implant to 10 days post-implant. The black arrow shows the first foci of ESCs and teratoma. D) Weight-curve of ESC-derived tumors. The red dashed line represents the average weight of drilled-plastic coverslip.

expression levels for several of the analyzed genes associated with endodermal and mesodermal lineages, exceptions being represented by *CXCR4*, *FoxA2*, *CD31*, *Adiponectin*, *Kdr* and *CD45* that were more expressed in CAM grafts than in EBs. Similarly, a higher expression of the genes associated with the ectodermal lineage were observed in teratomas when compared to EBs, including *Nestin*, *Nf2* and *Pax3*. Altogether, these data suggest that the presence of embryonic microenvironment may feed engrafted ESCs promoting their differentiation, highlighting the peculiar capacity of the chick embryo CAM to support ESCs differentiation.

3.3. Teratoma vasculature is the result of both vasculogenic and angiogenic events

Teratomas, as most of the solid tumors, recruit blood vessels from the surrounding tissues. Accordingly, ESC-derived teratoma grown onto CAM recruit vessels from the surrounding tissue through an angiogenic process easily visualized as large and small blood vessels penetrating inside the tumor mass (Fig. 4A). The presence of VEGFR2 immunoreactive cells inside teratoma sections confirm the molecular data shown in Fig. 3 and further support the occurrence of angiogenic events (Fig. 4B). However, in such samples, the possibility that some vessels may derive from the ESC differentiation cannot be excluded. To distinguish the avian ECs from the endothelium of murine origin, we selected two different antibodies with high species-specificity: an anti-PECAM1 antibody that labels murine ECs, and an anti-Von Willebrand Factor (FVIII) antibody that selectively recognizes avian ECs. ESC-derived teratomas were fixed in Zinc Fix solution and co-immunostained. Fig. 4C–D reveals the mosaic nature of newly formed blood vessels with ECs originating from both differentiated murine ESCs and the avian tissue. The presence of avian ECs ($FVIII^+$ cells) indicates the occurrence of angiogenic events, whereas murine $PECAM1^+$ cells represent differentiated elements derived from ESCs, likely generated by vasculogenesis. The overall appearance of the vasculature in teratomas grown onto the chick embryo CAM recalls the vessel network described in rapidly growing murine tumor models [34]. Some areas are well-vascularized, whereas other regions appear to be poorly vascularized and are flanked by sprouting neovessels (Fig. 4C).

To verify the ability of ECs from different origins to cooperate in the formation of perfused vessels, we analyze 15 μm slices of co-immunostained tumors using confocal microscopy. Intriguingly, several vascular structures composed of murine differentiated ECs are filled with nucleated avian erythrocytes (Fig. 5A), pointing to a connection of differentiated murine endothelium with the host vasculature. In addition, 3D reconstructions and orthogonal projections obtained from z-stack images reveal the presence of chimeric blood vessels

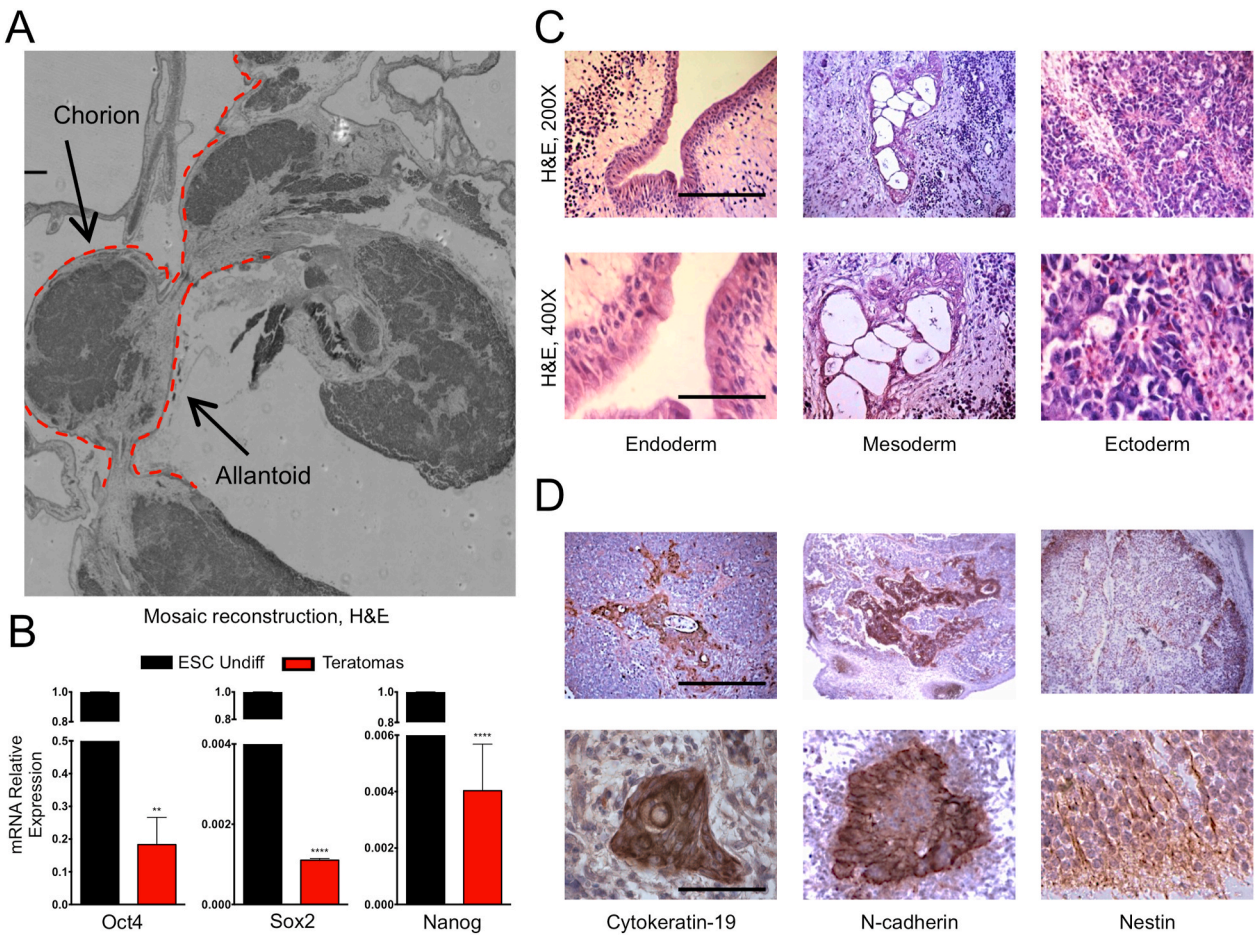

Fig. 2. Chick embryo CAM is able to support teratoma formation. A) Four μm sections of ES-derived teratoma were stained with Hematoxylin & Eosin. A whole section of teratoma grown on CAM was reconstructed using MosaicX module (AxioVision Software, Carl Zeiss). Black arrows and red dashed lines help to visualize epithelial cells monolayer belonging to chorion and allantoid. Scale bar 500 μm. B) mRNA expression levels of stemness genes were measured by RT-qPCR Data are the mean ± SEM of 4 independent samples and are expressed as relative expression ratios using one undifferentiated ESCs as reference **, $p < 0.01$; ****, $p < 0.001$, One-Way ANOVA followed by Bonferroni test versus control. C) Hematoxylin & Eosin stain of ES-derived tumors. Representative images of tissues derived from different germ layers. Ciliated epithelium (left), keratinized epithelium (centre), and neural rosette (right). (20 × top and 40 × bottom) B) Immunohistochemical analysis of ES-derived tumors for Cytokeratin-19, N-Cadherin, and Nestin in two different magnifications (20 × top - scale bar 200 μm, 40 × bottom - scale bar 50 μm). Images were acquired using a Zeiss Axio Imager.A2 microscope equipped with 20 × EC Plan-NEOFLUAR and 40 × EC Plan-NEOFLUAR objective.

formed by interconnected murine and avian ECs (Fig. 5B). The presence of nucleated chick red blood cells [35] inside the chimeric vessels suggests the patency and the functionality of these structures (Fig. 5C–D). Together these data confirm the co-presence of vasculogenic and angiogenic processes in ESC-derived teratomas grafted onto the CAM, similar to what observed in solid tumors [36]. On this basis, in order to define the kinetics of the occurrence of angiogenic and vasculogenic events during teratoma development, ESC-derived grafts were harvested at different were time points after grafting and analyzed by qPCR for the expression of avian and murine *CD31* transcripts. As anticipated, the tumor mass is nourished mainly by neovessels of chick origin during the first days of teratoma development as the consequence of angiogenic events that appear to decrease later on. At variance, the expression of murine *CD31* increases for the whole period of investigation, indicating that the vasculogenic process parallels the growth of the tumor mass (Fig. 5E).

4. Discussion

The CAM is a simple, quantifiable, and reproducible *in vivo* model valuable for cancer research. During CAM development, the vascular plexus derives from both angiogenic and vasculogenic events. In the early phases (before day 6 of development), angiogenic processes actively recruit mesodermal blood vessels towards the ectodermal basal lamina. Simultaneously, approximately between days 5 and 5.3 of development, vasculogenesis occurs from clusters of angioblasts located just below the ectodermal layer and around the mesodermal vascular plexus. Vessels that are arising from these angioblasts do not contain blood cells. However, at day 6, all vessels are pervious, indicating intercommunication of blood vessels arisen from both angiogenic and vasculogenic processes [37,38]. It is especially favored for the study of tumor angiogenesis because at the early stages of development, when generally tumor grafts are placed, the immune system is immature [10]. Thus, CAM well supports tumor cell grafting, growth, and colonization of distant tissues [39]. Several studies reported the engraftment of CAM with tumor cell lines, tumor biopsy specimens, and cell suspensions derived from mammalian tumors [40,41]. In these models, CAM allowed the characterization of pathways supporting tumor development and the analysis of the response of potential new therapeutic molecules [42]. Here we propose the chick embryo CAM as a natural scaffold for ESC differentiation, eligible for basic and translational researches. Murine ESCs engraft, grow, differentiate, and form a teratoma when implanted on CAM without the addition of exogenous stimuli. Already after 10 days, ES-derived teratomas reach a mass of approximately 450 mg composed of cells representing the three embryonic layers – endoderm, mesoderm, and ectoderm.

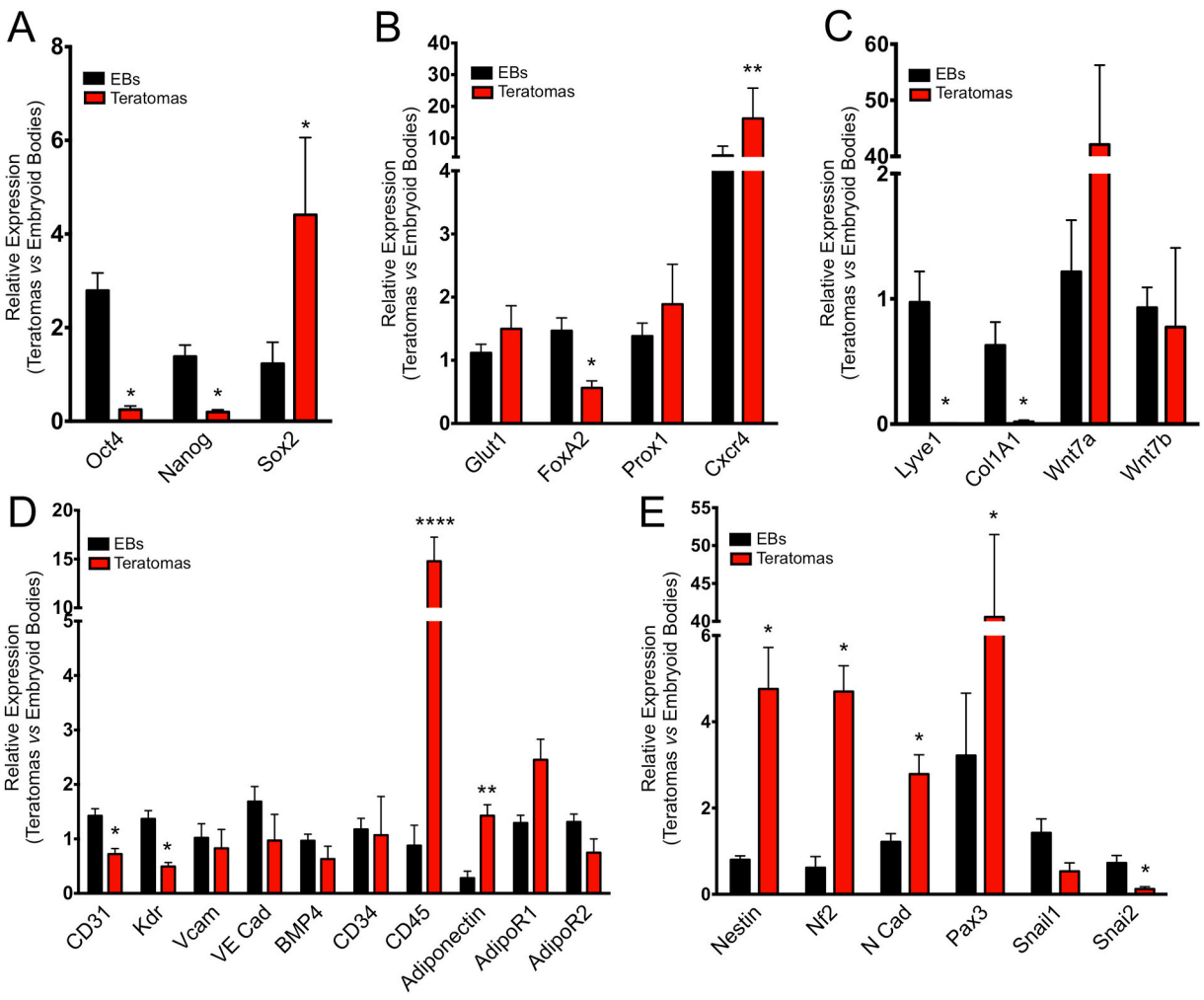

Fig. 3. Gene expression profile of ESC differentiation *in vitro* and *in vivo*. mRNA expression level of stemness genes (A), mesoderm-derived lineage (D), endoderm-derived lineage (B), ectoderm-derived tissues (E), and widespread-genes (C). Data are the mean ± SEM of 5–11 independent samples and are expressed as relative expression ratios using one ESC differentiated *in vitro* as reference. Data express the mean ± SEM of 5–11 independent differentiated samples. *, $p < 0.05$; **, $p < 0.01$; ****, $p < 0.0001$; One-Way ANOVA followed by Bonferroni's test versus control.

ESCs well adapt to the egg microenvironment. This should not be surprising since the eggs are an embryonic microenvironment enriched of all stimuli needed for embryonic development. In accordance, the expression of stemness genes *Oct4* and *Nanog* are more downregulated in CAM model respect to *in vitro* differentiation protocols, while the expression of *Sox2*, which reduces the self-renewal ability [43], is increased. Notably, some genes, mainly related to the ectodermal differentiation, appear to be differently expressed during the ESC differentiation *in vivo* when compared to their *in vitro* differentiation. Further studies will be required to assess the ability of the CAM microenvironment to drive ESC differentiation towards a particular lineage.

Compared to the classical ESC-derived teratoma assay in murine models, the CAM assay is less time-consuming. 10 days of differentiation are sufficient to generate a teratoma compared to 3–8 weeks needed in murine models [27]. In ESC-derived teratoma the angiogenic and vasculogenic events coexist and support the mass growth. During the first two days of differentiation, ESC form an avascularized mass. During differentiation, ESC release pro-angiogenic growth factors, including VEGF-A, IGF1, IGF2, PDGF, and FGF2 [44], that support the angiogenic growth of avian ECs. At 10 days avian vessels penetrating the mass are visible and support further ESC mass growth. At the same time, the vascular network of teratoma becomes enriched with murine ECs differentiated from implanted ESC through a vasculogesis-like process.

As observed in murine models [41] and during the early phases of CAM development [38], the vasculature of ESC-derived teratoma grown on the CAM contains chimeric host-/ESC-derived vessels originated by angiogenic and vasculogenic events that lead to functional chimeric vessels in which avian and murine ECs are anastomized.

The presence of chimeric vessels formed by host-derived endothelial cells and ECs differentiated from circulating endothelial cell precursors are found in many solid tumors where the angiogenic process can be flanked by the mobilization and differentiation of hematopoietic precursor cells [45,46]. Moreover, vascular mimicry events have been described in several malignant tumors such as melanoma and breast cancer, where tumor cells can participate in forming blood vessels. These tumor cells first transdifferentiate into stem cell-like cells and subsequently assume an endothelial-like phenotype, acquiring selective endothelial markers, and anticoagulant factors that allow the anastomosis with ECs [47,48]. Thus we propose the CAM model as a tool to analyze the process of tumor vascularization in terms of angiogenesis and vasculogenesis and their natural or synthetic positive and negative modulators.

5. Conclusion

The chicken CAM represents a perfect combination of multiple favorable factors. The embryonated eggs have an irrelevant cost; maintaining is simple and requires only a temperature-controlled box.

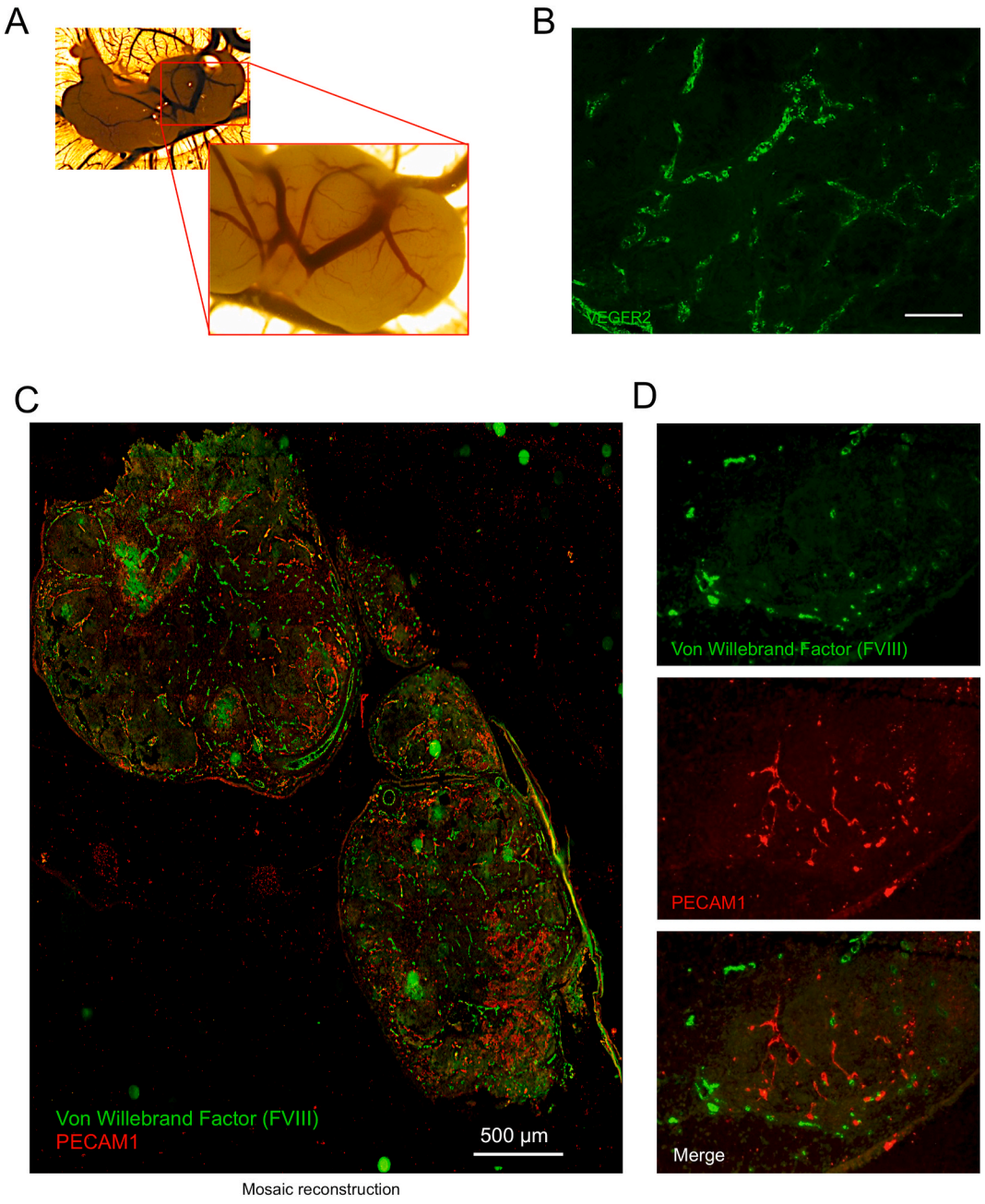

Fig. 4. The vascular system of ESC-derived teratomas. A) Representative Image of vessels penetrating into the teratoma, Whole teratoma were analyzed using a zoom microscope AXIO Zoom.V16. B) 4 μm FFPE sections were stained with anti-VEGFR2 antibody followed by AlexaFluor 488-conjugated secondary antibody to visualize the vasculature of the tumor. C) ES-derived tumors were fixed in Zinc Fix and 4 μm sections were stained with anti-von Willebrand Factor followed by AlexaFluor 488 and anti-mouse PECAM1 followed by AlexaFluor 594. A whole section of teratoma was reconstructed using MosaicX module. Scale bar 500 μm. D). 4 μm zinc fixed paraffin embedded sections of ES-derived tumors were stained with anti-von Willebrand Factor antibody followed by AlexaFluor 488-conjugated secondary antibody to visualize chicken vessels and anti-mouse PECAM1 antibody followed by AlexaFluor 594-conjugated secondary antibody to visualize differentiated murine ECs. Scale bar 50 μm. Pictures were acquired using a Zeiss Axiovert 200 M epifluorescence microscope equipped with 20 × EC Plan-NEOFLUAR objective.

Moreover, the surgical procedures do not require particularly expensive or elaborate equipment, including temperature, hydration control, or anesthesia. The identification of the CAM model as a substitute for mouse models perfectly reflects the "Replacement" purpose of the 3Rs law. The CAM is an accessible natural scaffold that supports ESC and tissue differentiation and may represent an essential tool for basic, pharmacological, regenerative studies and applied research.

Author contribution

Corsini Michela, Conceptualization, Formal analysis and Investigation, Writing – original draft, Ravelli Cosetta, Formal analysis and Investigation, Grillo Elisabetta, Formal analysis and Investigation, Dell'Era Patrizia, Formal analysis and Investigation, Presta Marco, Formal analysis and Investigation, Writing – original draft, Mitola Stefania, Formal analysis and Investigation, Conceptualization, Writing – original draft.

Founding

This work was supported by Associazione Italiana per la Ricerca sul Cancro (IG AIRC grant n° IG 17276 and AIRC grant n° IG 14395) to S.M

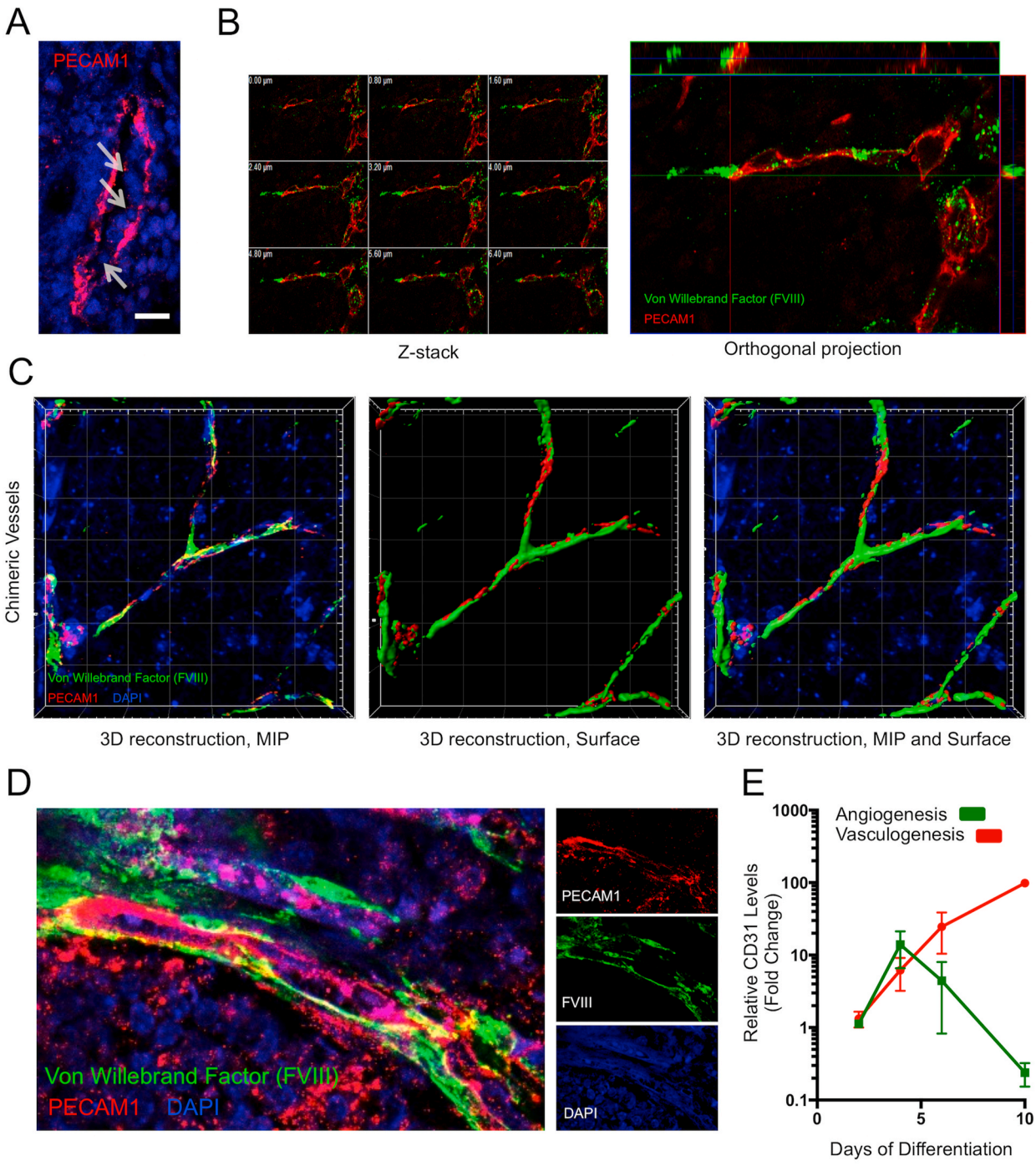

Fig. 5. The vascular system of ESC-derived teratomas is formed by functional interconnected vessels. A) 4 μm zinc fixed paraffin embedded sections of ESC-derived tumors were stained with anti-mouse. PECAM1 antibody followed by AlexaFluor 594-conjugated secondary antibody to visualize differentiated murine ECs. DAPI is used to counterstain nuclei. Arrows point to nucleated chick red blood cells within the murine PECAM1-positive vessel (Scale bar 20 μm .B) Z-stack sequence of 15 μm zinc fixed paraffin embedded teratoma. Avian ECs were stained with anti-von Willebrand Factor antibody followed by AlexaFluor 488-conjugated secondary antibody while murine-derived ECs were stained with anti-mouse PECAM1 antibody followed by AlexaFluor 594-conjugated secondary antibody (left panel). Orthogonal projection of Z-stack serie (right panel) highlights the connection between murine and avian vasculature (co-localized spots in yellow). C) Z-stack series of 15 μm zinc fixed paraffin embedded sections co-stained with anti-von Willebrand Factor antibody (green), anti-mouse PECAM1 antibody (red), and DAPI were acquired using a LSM510 Meta Confocal Microscope equipped with Plan-Apochromat 63 × /1.4 NA oil objectives and elaborated with IMARIS Image analysis software (Bitplane). Grid scale bar 20 μm. C) Detail of 4 μm zinc fixed paraffin embedded section co-stained with anti-von Willebrand Factor antibody (green), anti-mouse PECAM1 antibody (red) and DAPI (blue) shows nucleated red blood cells into chimeric vessels. E) Time course analysis of avian and murine CD31 expression levels during teratoma formation.

and M.P.; E.G. was supported by Veronesi fellowships; MPP Lab was supported by Fondazione Cariplo and Regione Lombardia.

Declaration of competing interest

All authors declare no conflict of interest.

References

[1] S. Patan, Vasculogenesis and angiogenesis, Canc. Treat Res. 117 (2004) 3–32.
[2] D.G. Duda, K.S. Cohen, S.V. Kozin, J.Y. Perentes, D. Fukumura, D.T. Scadden, R. K. Jain, Evidence for incorporation of bone marrow-derived endothelial cells into perfused blood vessels in tumors, Blood 107 (2006) 2774–2776.
[3] S. Guelfi, H. Duffau, L. Bauchet, B. Rothhut, J.P. Hugnot, Vascular transdifferentiation in the CNS: a focus on neural and glioblastoma stem-like cells, Stem Cell. Int. 2016 (2016) 2759403.
[4] E. Lizarraga-Verdugo, M. Avendano-Felix, M. Bermudez, R. Ramos-Payan, C. Perez-Plasencia, M. Aguilar-Medina, Cancer stem cells and its role in angiogenesis and vasculogenic mimicry in gastrointestinal cancers, Frontiers in oncology 10 (2020) 413.
[5] E.A. Ober, H.A. Field, D.Y. Stainier, From endoderm formation to liver and pancreas development in zebrafish, Mech. Dev. 120 (2003) 5–18.
[6] S. Cermenati, S. Moleri, S. Cimbro, P. Corti, L. Del Giacco, R. Amodeo, E. Dejana, P. Koopman, F. Cotelli, M. Beltrame, Sox18 and Sox7 play redundant roles in vascular development, Blood 111 (2008) 2657–2666.
[7] M.N. Vergara, M.V. Canto-Soler, Rediscovering the chick embryo as a model to study retinal development, Neural Dev. 7 (2012) 22.
[8] J.G. Vilches-Moure, Embryonic chicken (Gallus gallus domesticus) as a model of cardiac biology and development, Comp. Med. 69 (2019) 184–203.
[9] B.L. Roman, B.M. Weinstein, Building the vertebrate vasculature: research is going swimmingly, Bioessays 22 (2000) 882–893.
[10] D. Ribatti, The chick embryo chorioallantoic membrane as a model for tumor biology, Exp. Cell Res. 328 (2014) 314–324.
[11] P.M. Kulesa, C.M. Bailey, C. Cooper, S.E. Fraser, In ovo live imaging of avian embryos, Cold Spring Harb. Protoc. 6 (2010) (2010) (2010) pdb prot5446.
[12] D. Ribatti, The chick embryo chorioallantoic membrane (CAM). A multifaceted experimental model, Mech. Dev. 141 (2016) 70–77.
[13] V. Hamburger, H.L. Hamilton, A series of normal stages in the development of the chick embryo, J. Morphol. 88 (1951) 49–92.
[14] I. Moreno-Jimenez, G. Hulsart-Billstrom, S.A. Lanham, A.A. Janeczek, N. Kontouli, J.M. Kanczler, N.D. Evans, R.O. Oreffo, The chorioallantoic membrane (CAM) assay for the study of human bone regeneration: a refinement animal model for tissue engineering, Sci. Rep. 6 (2016) 32168.
[15] G. Andres, D. Leali, S. Mitola, D. Coltrini, M. Camozzi, M. Corsini, M. Belleri, E. Hirsch, R.A. Schwendener, G. Christofori, A. Alcami, M. Presta, A pro-inflammatory signature mediates FGF2-induced angiogenesis, J. Cell Mol. Med. 13 (2009) 2083–2108.
[16] A. Woloszyk, D. Liccardo, T.A. Mitsiadis, Three-dimensional imaging of the developing vasculature within stem cell-seeded scaffolds cultured in ovo, Front. Physiol. 7 (2016) 146.
[17] C. Ravelli, S. Mitola, M. Corsini, M. Presta, Involvement of alphavbeta3 integrin in gremlin-induced angiogenesis, Angiogenesis 16 (2013) 235–243.
[18] S. Rezzola, M. Di Somma, M. Corsini, D. Leali, C. Ravelli, V.A.B. Polli, E. Grillo, M. Presta, S. Mitola, VEGFR2 activation mediates the pro-angiogenic activity of BMP4, Angiogenesis 22 (2019) 521–533.
[19] M.I. Nawaz, S. Rezzola, C. Tobia, D. Coltrini, M. Belleri, S. Mitola, M. Corsini, A. Sandomenico, A. Caporale, M. Ruvo, M. Presta, D-Peptide analogues of Boc-Phe-Leu-Phe-Leu-Phe-COOH induce neovascularization via endothelial N-formyl peptide receptor 3, Angiogenesis (2020).
[20] D. Ribatti, R. Tamma, The chick embryo chorioallantoic membrane as an in vivo experimental model to study human neuroblastoma, J. Cell. Physiol. 234 (2018) 152–157.
[21] C.E. Murry, G. Keller, Differentiation of embryonic stem cells to clinically relevant populations: lessons from embryonic development, Cell 132 (2008) 661–680.
[22] S.N. Hassani, S. Moradi, S. Taleahmad, T. Braun, H. Baharvand, Transition of inner cell mass to embryonic stem cells: mechanisms, facts, and hypotheses, Cell. Mol. Life Sci. 76 (2019) 873–892.
[23] T. Boroviak, R. Loos, P. Bertone, A. Smith, J. Nichols, The ability of inner-cell-mass cells to self-renew as embryonic stem cells is acquired following epiblast specification, Nat. Cell Biol. 16 (2014) 516–528.
[24] T. Vazin, W.J. Freed, Human embryonic stem cells: derivation, culture, and differentiation: a review, Restor. Neurol. Neurosci. 28 (2010) 589–603.
[25] E. Crescini, L. Gualandi, D. Uberti, C. Prandelli, M. Presta, P. Dell'Era, Ascorbic acid rescues cardiomyocyte development in Fgfr1(-/-) murine embryonic stem cells, Biochim. Biophys. Acta 1833 (2013) 140–147.
[26] R. Ronca, L. Gualandi, E. Crescini, S. Calza, M. Presta, P. Dell'Era, Fibroblast growth factor receptor-1 phosphorylation requirement for cardiomyocyte differentiation in murine embryonic stem cells, J. Cell Mol. Med. 13 (2009) 1489–1498.
[27] H. Hentze, P.L. Soong, S.T. Wang, B.W. Phillips, T.C. Putti, N.R. Dunn, Teratoma formation by human embryonic stem cells: evaluation of essential parameters for future safety studies, Stem Cell Res. 2 (2009) 198–210.
[28] R.V. Nelakanti, N.G. Kooreman, J.C. Wu, Teratoma formation: a tool for monitoring pluripotency in stem cell research, Curr Protoc Stem Cell Biol 32 (2015) 4A 8 1–4A 8 17.
[29] C.X. Deng, A. Wynshaw-Boris, M.M. Shen, C. Daugherty, D.M. Ornitz, P. Leder, Murine FGFR-1 is required for early postimplantation growth and axial organization, Genes Dev. 8 (1994) 3045–3057.
[30] M. Corsini, E. Moroni, C. Ravelli, E. Grillo, M. Presta, S. Mitola, In situ DNA/protein interaction assay to visualize transcriptional factor Activation, Methods and protocols 3 (2020).
[31] J. Rossant, V.E. Papaioannou, The relationship between embryonic, embryonal carcinoma and embryo-derived stem cells, Cell Differ. 15 (1984) 155–161.
[32] N.S. Hwang, S. Varghese, J. Elisseeff, Controlled differentiation of stem cells, Adv. Drug Deliv. Rev. 60 (2008) 199–214.
[33] M.C. Simon, B. Keith, The role of oxygen availability in embryonic development and stem cell function, Nat. Rev. Mol. Cell Biol. 9 (2008) 285–296.
[34] Z. Li, H. Huang, P. Boland, M.G. Dominguez, P. Burfeind, K.M. Lai, H.C. Lin, N. W. Gale, C. Daly, W. Auerbach, D. Valenzuela, G.D. Yancopoulos, G. Thurston, Embryonic stem cell tumor model reveals role of vascular endothelial receptor tyrosine phosphatase in regulating Tie2 pathway in tumor angiogenesis, Proc. Natl. Acad. Sci. U. S. A. 106 (2009) 22399–22404.
[35] D. Bronnimann, T. Annese, T.A. Gorr, V. Djonov, Splitting of circulating red blood cells as an in vivo mechanism of erythrocyte maturation in developing zebrafish, chick and mouse embryos, J. Exp. Biol. 221 (2018).
[36] Y. Yi, I.Y. Hsieh, X. Huang, J. Li, W. Zhao, Glioblastoma stem-like cells: characteristics, microenvironment, and therapy, Front. Pharmacol. 7 (2016) 477.
[37] D. Ribatti, L. Roncali, B. Nico, M. Bertossi, Effects of exogenous heparin on the vasculogenesis of the chorioallantoic membrane, Acta Anat. 130 (1987) 257–263.
[38] G. Melkonian, C. Le, W. Zheng, P. Talbot, M. Martins-Green, Normal patterns of angiogenesis and extracellular matrix deposition in chick chorioallantoic membranes are disrupted by mainstream and sidestream cigarette smoke, Toxicol. Appl. Pharmacol. 163 (2000) 26–37.
[39] F. Maule, S. Bresolin, E. Rampazzo, D. Boso, A. Della Puppa, G. Esposito, E. Porcu, S. Mitola, G. Lombardi, B. Accordi, M. Tumino, G. Basso, L. Persano, Annexin 2A sustains glioblastoma cell dissemination and proliferation, Oncotarget 7 (2016) 54632–54649.
[40] M.R. Lowerison, C. Huang, F. Lucien, S. Chen, P. Song, Ultrasound localization microscopy of renal tumor xenografts in chicken embryo is correlated to hypoxia, Sci. Rep. 10 (2020) 2478.
[41] J. Hu, M. Ishihara, A.I. Chin, L. Wu, Establishment of xenografts of urological cancers on chicken chorioallantoic membrane (CAM) to study metastasis, Precis Clin Med 2 (2019) 140–151.
[42] S. Rezzola, M. Dal Monte, M. Belleri, A. Bugatti, P. Chiodelli, M. Corsini, M. Cammalleri, A. Cancarini, L. Morbidelli, P. Oreste, P. Bagnoli, F. Semeraro, M. Presta, Therapeutic potential of anti-angiogenic multitarget N,O-sulfated E. Coli K5 polysaccharide in diabetic retinopathy, Diabetes 64 (2015) 2581–2592.
[43] J.L. Kopp, B.D. Ormsbee, M. Desler, A. Rizzino, Small increases in the level of Sox2 trigger the differentiation of mouse embryonic stem cells, Stem Cell. 26 (2008) 903–911.
[44] A.V. Ngangan, J.C. Waring, M.T. Cooke, C.J. Mandrycky, T.C. McDevitt, Soluble factors secreted by differentiating embryonic stem cells stimulate exogenous cell proliferation and migration, Stem Cell Res. Ther. 5 (2014) 26.
[45] R. Ria, C. Piccoli, T. Cirulli, F. Falzetti, G. Mangialardi, D. Guidolin, A. Tabilio, N. Di Renzo, A. Guarini, D. Ribatti, F. Dammacco, A. Vacca, Endothelial differentiation of hematopoietic stem and progenitor cells from patients with multiple myeloma, Clin. Canc. Res. 14 (2008) 1678–1685.
[46] P. Fons, J.P. Herault, N. Delesque, J. Tuyaret, F. Bono, J.M. Herbert, VEGF-R2 and neuropilin-1 are involved in VEGF-A-induced differentiation of human bone marrow progenitor cells, J. Cell. Physiol. 200 (2004) 351–359.
[47] J.M. Dunleavey, A.C. Dudley, Vascular mimicry: concepts and implications for anti-angiogenic therapy, Curr. Antimicrob. 1 (2012) 133–138.
[48] A.J. Maniotis, R. Folberg, A. Hess, E.A. Seftor, L.M. Gardner, J. Pe'er, J.M. Trent, P. S. Meltzer, M.J. Hendrix, Vascular channel formation by human melanoma cells in vivo and in vitro: vasculogenic mimicry, Am. J. Pathol. 155 (1999) 739–752.